Application of the Energy-Casimir Method to the Study of Mesoscale Disturbance Stability*

RAN Lingkun[1†](冉令坤), CHU Yanli[2](楚艳丽), and GAO Shouting[1](高守亭)

1 *Institute of Atmospheric Physics, Chinese Academy of Sciences, Beijing* 100029

2 *Institute of Urban Meteorology, China Meteorological Administration, Beijing* 100089

(Received February 2, 2009)

ABSTRACT

Taking into account the effect of moisture, we derive a three-dimensional pseudoenergy wave-activity relation for moist atmosphere from the primitive zonal momentum and total energy equations in Cartesian coordinates by using the energy-Casimir method. In the derivation, a Casimir function is introduced, which is a single-value function of virtual potential temperature. Since the pseudoenergy wave-activity relation is constructed in the ageostrophic and nonhydrostatic dynamical framework, it may be applicable to diagnosing the stability of mesoscale disturbance systems in a steady-stratified atmosphere. The theoretical analysis shows that the wave-activity relation takes a nonconservative form in which the pseudoenergy wave-activity density is composed of perturbation kinetic energy, available potential energy, and buoyant energy. The local change of pseudoenergy wave-activity density depends on the combined effects of zonal basic flow shear, Coriolis force work and wave-activity source or sink as well as wave-activity flux divergence. The diagnosis shows that horizontal distribution and temporal trend of pseudoenergy wave-activity density are similar to those of the observed 6-h accumulated surface rainfall. This suggests that the pseudoenergy wave-activity density is capable of representing the dynamical and thermodynamic features of mesoscale precipitable systems in the mid-lower troposphere, so it is closely related to the observed surface rainfall. The calculation of the terms in the wave-activity relation reveals that the wave-activity flux divergence shares a similar temporal trend with the local change of pseudoenergy wave-activity density and the observed surface rainfall. Although the terms of zonal basic flow shear and Coriolis force contribute to the local change of pseudoenergy wave-activity density, the contribution from the wave-activity flux divergence is much more significant.

Key words: pseudoenergy wave-activity density, wave-activity flux, steady stratification, stability

Citation: Ran Lingkun, Chu Yanli, and Gao Shouting, 2010: Application of the energy-Casimir method to the study of mesoscale disturbance stability. *Acta Meteor. Sinica*, **24**(3), 297–306.

1. Introduction

Stability is a key research topic in the geostrophic fluid dynamics. Meteorologists have done a number of outstanding works in the stability-related research. They extended the investigation from linear system to weak nonlinear and nonlinear ones, from conservative system to dissipative ones. For example, Kuo (1949) firstly applied the Rayleigh theorem to analysis of rotational atmosphere, and obtained the necessary condition for instability of barotropic atmosphere. Charney (1947) and Eady (1949) proposed the theory of baroclinic stability. Stone (1966) studied the symmetric instability and Kelvin-Helmholtz instability, and set up a stability criterion in virtual of the Richardson number. Gao and Sun (1986) and Gao et al. (1990) examined the instability of mesoscale disturbances and discussed the dynamic mechanisms of jet stream acceleration and low-level frontgenesis. Taking into account friction and terrain, Lu (1989) used the Serrin-Joseph energy method to derive the nonlinear stability criterion for shearing basic flow. Huang and Zhang (2008) depicted the dynamic instability of spiral cloud bands of tropic cyclones. Zhou et al. (2003) analyzed the favorable conditions of convective instability and conditional symmetric instability. Shen et al. (2007) investigated the oblique-cross instability of zonal linear disturbance moving at an arbitrary angle with basic

*Supported by the National Basic Research Program of China under Grant No. 2009CB421505 and the National Natural Sciences Foundation of China under Grant Nos. 40875032, 40405011 and 40475006.

†Corresponding author: rlk@mail.iap.ac.cn.

(Chinese version published in Vol. 67, No. 4, 530–539, 2009)

flow, and his results showed that 1) the oblique-cross instability of linear shear basic flow was caused by internal inertial gravity waves, and 2) the oblique-cross instability of non-linear second-order shear basic flow included internal inertial gravity wave as well as vortex-Rossby wave. Ding and Shen (1998) discussed the symmetric instabilities of non-zonal and non-parallel mean flows and arrived at the symmetric instability criteria of disturbance to irrotational stratified flow. Exploiting the two-demensional non-hydrostatic balance model, Zhang and Zhang (1995) simulated the linear and non-linear instability, and pointed out that when the disturbance grew to a certain degree, the contribution of advection would destroy the structure of symmetric circulation and could not be ignored.

The energy-Casimir method, developed by Arnol'd in the 1960s, is one of the most important approaches to study non-linear stability since the 1980s. Arnol'd (1965, 1966) combined variation principle with priori estimate (also known as integral estimate) to investigate the non-linear stability of two-dimensional, inviscid and incompressible fluid, and set up two non-linear stability criteria, namely, Arnol'd first theorem and second theorem. The method he employed is called the Arnol'd method, hereafter referred to as the "energy-Casimir method". On the basis of the Arnol'd method, Zeng (1989) proposed a general variation method, and constructed a series of non-linear stability criteria for barotropic and baroclinic quasi-geostrophic models, layered models, and primitive equation models. Mu (1991, 1992, 1998) further developed the energy-Casimir method and established the two-dimensional barotropic quasi-geostrophic model and the general multi-layer quasi-geostrophic model, as well as the the stability criteria for non-linear and three-dimensional continuous stratification quasigeostrophic motion (Mu and Zeng, 1991; Mu and Wang, 1992; Li and Mu, 1996; Liu and Mu, 1994). In addition, Mu et al. (1999) discussed the upper-bound estimate and saturation problem of disturbance. Ren (2000) worked on finite-amplitude wave-activity invariants for semi-geostrophic shallow water equations and put forward the non-linear instability criteria.

Another important application of the energy-Casimir method is to construct wave-activity relation, a useful tool for diagnosing wave stability. The method's kernel idea is that one selects a Casimir function C (a function of some conservative quantity η, namely $C(\eta)$) to make the perturbation part $\frac{1}{2}|\boldsymbol{v}_0+\boldsymbol{v}_\mathrm{e}|^2-\frac{1}{2}|\boldsymbol{v}_0|^2+C(\eta_0+\eta_\mathrm{e})-C(\eta_0)$(where the subscript "0" denotes the basic state, "e" represents the disturbance) of the Hamilton invariant $\frac{1}{2}|\boldsymbol{v}|^2+C(\eta)$ be the sum of the quadratic perturbation amplitude term and the leading-order perturbation divergence term. A wave-activity relation may be yielded by putting the sum into the equation of Hamilton invariant as follows

$$\frac{\partial A}{\partial t}+\nabla\cdot\boldsymbol{F}=S,$$

where A is the wave-activity density, $\boldsymbol{F}$ the wave-activity flux, and S the source or sink. The wave-activity relation is widely used for wave stability as well as interaction between wave and basic flow. For small-amplitude disturbances, both A and $\boldsymbol{F}$ are quadratic in the perturbation field. If the sign of A is definitive, the wave-activity relation, capable of indicating local convergence and local divergence of perturbation energy, may serve for diagnosing disturbance stability. By using the quasi-geostrophic barotropic equation, McIntyre and Shepherd (1987) studied the wave-activity conservation equation for the finite-amplitude disturbance in non-parallel sheared flows. Banishing the dynamic constraint condition of Hamilton system and including forcing and dissipation, Haynes (1988) derived a finite-amplitude wave-activity relation for zonal and non-zonal symmetric basic flow on the basis of McIntyre and Shepherd (1987).

In the previous research, the energy-Casimir method was mainly applied to the quasi-geostrophic and hydrostatic dynamic systems in dry air without consideration of water vapor. Consequently, the obtained results were only suitable for large scale systems, but not for non-hydrostatic mesoscale systems leading to torrential rain. The application of the energy-Casimir method to mesoscale systems in moist air is few. So it is thought that a further investigation of the energy-Casimir method for mesoscale stability may give some new insight into the evolution of mesoscale systems. Following this consideration, we employ the energy-Casimir method to derive the pseudoenergy wave-activity relation for moist air in this paper and further apply it to diagnosing the stability of mesoscale disturbances in a steady-stratified basic flow.

2. Governing equations

For diabatic, frictionless, nonhydrostatic, compressible, and rotating moist atmosphere, the governing equations in Cartesian coordinates may be given by

$$\frac{\partial u}{\partial t}+\boldsymbol{v}\cdot\nabla u-fv=-\frac{1}{\rho}\frac{\partial p}{\partial x}, \tag{1}$$

$$\frac{\partial v}{\partial t}+\boldsymbol{v}\cdot\nabla v+fu=-\frac{1}{\rho}\frac{\partial p}{\partial y}, \tag{2}$$

$$\frac{\partial w}{\partial t}+\boldsymbol{v}\cdot\nabla w=-\frac{1}{\rho}\frac{\partial p}{\partial z}-g, \tag{3}$$

$$\frac{\partial \rho}{\partial t}+\nabla\cdot(\rho\boldsymbol{v})=0, \tag{4}$$

$$\frac{\partial \theta}{\partial t}+\boldsymbol{v}\cdot\nabla\theta=\frac{\theta}{c_pT}Q, \tag{5}$$

$$\frac{\partial q_v}{\partial t}+\boldsymbol{v}\cdot\nabla q_v=S_{q_v}, \tag{6}$$

$$p=\rho RT(1+\lambda q_v), \tag{7}$$

$$\theta=T\Big(\frac{p_s}{p}\Big)^{\frac{R}{c_p}}, \tag{8}$$

where $\boldsymbol{v}=(u,v,w)$ is the three-dimensional velocity vector, q_v the specific humidity, Q the diabatic heating rate, $\lambda=0.61$ a constant, S_{q_v} the source or sink of water vapor, and other symbols are conventional in meteorology. Combining the mass-continuity Eq. (4), thermodynamic Eq. (5), and water vapor Eq. (6) with the definition of potential temperature (Eq. (8)), one may obtain the equations for virtual temperature and virtual potential temperature

$$\frac{\partial \ln T_v}{\partial t}+\boldsymbol{v}\cdot\nabla \ln T_v=-\frac{R}{c_v}\nabla\cdot\boldsymbol{v} +\frac{1}{c_v}\Big(\frac{Q}{T}+\lambda c_p\frac{T}{T_v}S_{q_v}\Big), \tag{9}$$

$$\frac{\partial \theta_v}{\partial t}+\boldsymbol{v}\cdot\nabla\theta_v=\theta_v\Big(\frac{Q}{c_pT}+\lambda\frac{T}{T_v}S_{q_v}\Big), \tag{10}$$

where $T_v=T(1+\lambda q_v)$ represents the virtual temperature, and $\theta_v=T_v\Big(\frac{p_s}{p}\Big)^{\frac{R}{c_p}}$ is the virtual potential temperature. By using Eqs. (1)–(4) and (9), the total energy equation may be given by

$$\frac{\partial}{\partial t}(\rho E)+\nabla\cdot[\boldsymbol{v}(\rho E+p)]=\rho[(1+\lambda q_v)Q +\lambda c_pTS_{q_v}], \tag{11}$$

where the total energy density ($E=\frac{1}{2}(u^2+v^2+w^2)+gz+c_vT_v$) is the sum of kinetic energy ($\frac{1}{2}(u^2+v^2+w^2)$), potential energy (gz), and internal energy (c_vT_v). It is shown that the total energy of moist air is nonconservative due to the two terms on the right-hand side (RHS) of Eq. (11), namely diabatic heating (the first term) and source or sink of water vapor (the second term).

To derive the pseudoenergy wave-activity relation with the energy-Casimir method, a Casimir function, which is a single function of virtual potential temperature, namely, $C=C(\theta_v)$, is introduced. In virtual of Eq. (10), the Casimr function is proved to satisfy the following equation

$$\frac{\partial}{\partial t}(\rho C)+\nabla\cdot(\rho\boldsymbol{v}C)=\rho\theta_v\frac{\mathrm{d}C}{\mathrm{d}\theta_v}\Big(\frac{Q}{c_pT}+\lambda\frac{T}{T_v}S_{q_v}\Big). \tag{12}$$

Combination of Eq. (1) with Eqs. (11) and (12) may yield

$$\begin{aligned}&\frac{\partial}{\partial t}\left\{\rho\left[E-u_0\Big(u-\frac{u_0}{2}\Big)+C\right]\right\}\\&+\nabla\cdot\left\{\boldsymbol{v}\rho\left[E-u_0(u-\frac{u_0}{2})+C\right]+\boldsymbol{v}p\right\}\\&=u_0\frac{\partial p}{\partial x}+\rho\left[(u_0-u)\left(v\frac{\partial u_0}{\partial y}+w\frac{\partial u_0}{\partial z}\right)\right.\\&\left.-u_0fv\right]+\rho\Big(\frac{T_v}{T}\frac{Q}{c_p}+\lambda TS_{q_v}\Big)\Big(\frac{\mathrm{d}C}{\mathrm{d}\theta_v}\frac{\theta_v}{T_v}+c_p\Big),\end{aligned} \tag{13}$$

where $u_0=u_0(y,z)$ is the zonal basic flow.

In the following section, Eq. (13) is adopted to derive the pseudoenergy wave-activity relation, which is suitable for investigating mesoscale stability.

3. The pseudoenergy wave-activity relation

Supposing all variables consist of basic-state parts and perturbation parts, thus

$$\begin{pmatrix} u \\ v \\ w \\ p \\ T \\ \rho \\ \theta \end{pmatrix} = \begin{pmatrix} u_0 + u_{\rm e} \\ v_{\rm e} \\ w_{\rm e} \\ p_0 + p_{\rm e} \\ T_0 + T_{\rm e} \\ \rho_0 + \rho_{\rm e} \\ \theta_0 + \theta_{\rm e} \end{pmatrix}, \tag{14}$$

where the subscripts “0” and “e” represent the basic state and the perturbation, respectively. Note that the meridional and vertical components of velocity at basic state are zero, namely, $v_0 = 0$ and $w_0 = 0$, and the other basic-state quantities are the function of y and z. The basic states satisfy the following relations

$$fu_0 = -\frac{1}{\rho_0}\frac{\partial p_0}{\partial y}, \tag{15}$$

$$\frac{\partial p_0}{\partial z} = -\rho_0 g, \tag{16}$$

$$p_0 = \rho_0 R T_{v0}, \tag{17}$$

$$\theta_{v0} = T_{v0}\Big(\frac{p_s}{p_0}\Big)^{\frac{R}{c_p}}. \tag{18}$$

Since the inequalities $\left|\frac{\theta_{ve}}{\theta_{v0}}\right| < 1$, $\left|\frac{\rho_{\rm e}}{\rho_0}\right| < 1$, $\left|\frac{T_{ve}}{T_{v0}}\right| < 1$, and $\left|\frac{p_{\rm e}}{p_0}\right| < 1$ hold in general case, the linear relation between perturbation thermodynamic quantities may be derived from Eqs. (7) and (8)

$$\frac{p_{\rm e}}{p_0} \approx \frac{\rho_{\rm e}}{\rho_0} + \frac{T_{ve}}{T_{v0}}, \tag{19}$$

$$\frac{\theta_{ve}}{\theta_{v0}} \approx \frac{T_{ve}}{T_{v0}} - \frac{R}{c_p}\frac{p_{\rm e}}{p_0}. \tag{20}$$

The approximate expression of T_{ve} can be obtained by eliminating $\frac{p_{\rm e}}{p_0}$ from the above two equations

$$T_{ve} \approx \frac{c_p}{c_v}\frac{T_{v0}}{\theta_{v0}}\theta_{ve} + \frac{R}{c_v}\frac{T_{v0}}{\rho_0}\rho_{\rm e}. \tag{21}$$

By performing Taylor series expansion on Casimir function at $\theta_v = \theta_{v0}$, and omitting the three-order and higher-order contributions, one may rewrite $C(\theta_v)$ approximately as

$$C(\theta_v) = C_0 + \frac{{\rm d}C_0}{{\rm d}\theta_{v0}}\theta_{ve} + \frac{1}{2}\frac{{\rm d}^2 C_0}{{\rm d}\theta_{v0}^2}\theta_{ve}^2, \tag{22}$$

where $C_0 = C(\theta_{v0})$ is the basic-state Casimir function. After substituting Eqs. (14) and (22) into the quantity $\rho\Big[E - u_0\Big(u - \frac{u_0}{2}\Big) + C\Big]$, one has

$$\begin{aligned}
&\rho\Big[E - u_0\Big(u - \frac{u_0}{2}\Big) + C\Big] \\
&= \rho_0(c_v T_{v0} + gz + C_0) + \rho_0\Big(\frac{{\rm d}C_0}{{\rm d}\theta_{v0}} + \frac{T_{v0}c_p}{\theta_{v0}}\Big)\theta_{ve} \\
&\quad + \rho_{\rm e}(c_p T_{v0} + gz + C_0) + p_0\Big(\frac{\rho_{\rm e}}{\rho_0}\Big)^2 + \frac{\rho_0}{2}\Big(u_{\rm e}^2 + v_{\rm e}^2 \\
&\quad + w_{\rm e}^2 + \frac{{\rm d}^2 C_0}{{\rm d}\theta_{v0}^2}\theta_{ve}^2\Big) + \Big(\frac{{\rm d}C_0}{{\rm d}\theta_{v0}} + \frac{T_{v0}c_p}{\theta_{v0}}\Big)\rho_{\rm e}\theta_{ve}.
\end{aligned} \tag{23}$$

According to the kernel idea of the energy-Casimir method, in order to write Eq. (23) as the sum of basic-state terms and quadric-order perturbation terms, we choose C_0 to satisfy the following relation

$$c_p T_{v0} + gz + C_0 = 0. \tag{24}$$

Taking partial derivative with respect to z to Eq. (24), and applying the equation $\frac{\partial\theta_{v0}}{\partial z} = \frac{\theta_{v0}}{T_{v0}}\Big(\frac{\partial T_{v0}}{\partial z} + \frac{R}{c_p}g\Big)$, one may obtain

$$\frac{{\rm d}C_0}{{\rm d}\theta_{v0}} = -\frac{c_p T_{v0}}{\theta_{v0}}, \tag{25}$$

$$\frac{{\rm d}^2 C_0}{{\rm d}\theta_{v0}^2} = \frac{g}{\theta_{v0}\dfrac{\partial\theta_{v0}}{\partial z}}. \tag{26}$$

With the substitution of Eqs. (24)–(26), Eq. (23) becomes

$$\rho\Big[E - u_0\Big(u - \frac{u_0}{2}\Big) + C\Big] = A - p_0, \tag{27}$$

where $A = \frac{\rho_0}{2}\Big(u_{\rm e}^2 + v_{\rm e}^2 + w_{\rm e}^2 + \frac{g}{\theta_{v0}\frac{\partial\theta_{v0}}{\partial z}}\theta_{ve}^2\Big) + p_0\Big(\frac{\rho_{\rm e}}{\rho_0}\Big)^2$ is the pseudoenergy wave-activity density, which is the sum of perturbation kinetic energy $\frac{\rho_0}{2}(u_{\rm e}^2 + v_{\rm e}^2 + w_{\rm e}^2)$, available potential energy $\frac{\rho_0}{2}\frac{g}{\theta_{v0}\frac{\partial\theta_{v0}}{\partial z}}\theta_{ve}^2$ and buoyant energy $p_0\Big(\frac{\rho_{\rm e}}{\rho_0}\Big)^2$. It is emphasized that Eq. (27) holds under the condition that C_0 satisfies Eq. (24).

Substituting Eqs. (14) and (27) into Eq. (13), and omitting the three-order contribution, one may obtain the pseudoenergy wave-activity relation as follows

$$\frac{\partial A}{\partial t}+\nabla\cdot\boldsymbol{F}$$
$$=-\rho_0u_{\rm e}\Big(v_{\rm e}\frac{\partial u_0}{\partial y}+w_{\rm e}\frac{\partial u_0}{\partial z}\Big)-\rho u_0fv_{\rm e}$$
$$+\rho\Big(\frac{T_v}{T}\frac{Q}{c_p}+\lambda TS_{qv}\Big)\Big(\frac{{\rm d}C}{{\rm d}\theta_v}\frac{\theta_v}{T_v}+c_p\Big),\qquad(28)$$

where the three-dimensional vector

$$\boldsymbol{F}=\begin{pmatrix}u_0A+u_{\rm e}p_{\rm e}\\ v_{\rm e}p_{\rm e}\\ w_{\rm e}p_{\rm e}\end{pmatrix}$$

is quadric in perturbation amplitude, and is called pseudoenergy wave-activity flux. Built up in the non-hydrostatic dynamic framework, Eq. (28) is suitable for mesoscale systems. The pseudoenergy wave-activity density for moist atmosphere is nonconservative due to the contributions of zonal basic flow shear (the first term of RHS of Eq. (28)), Coriolis force work (the second term of RHS), and source or sink due to diabatic heating and water vapor phase change (the third term of RHS). Since the terms associated with zonal basic flow shear, Coriolis force work, and u_0A couple perturbation vortex with basic flow, they represent the influence of basic flow on tendency of pseudoenergy wave-activity density.

We have to emphasize that if the basic flow is under steady stratification ($\frac{\partial\theta_0}{\partial z}>0$), A is always positive, indicating that A increases as mesoscale system develops, while A decreases due to the decay of mesoscale system. If the flow is under unsteady stratification ($\frac{\partial\theta_0}{\partial z}<0$), A is either negative or positive. In this case, A is indefinite in sign for developing mesoscale system. The increase or decrease of A depends on the difference of perturbation kinetic energy, buoyant energy, and available potential energy. For this situation, A cannot indicate the evolvement of mesoscale system.

If the basic flow is under steady stratification, the convergence of wave-activity flux ($\nabla\cdot\boldsymbol{F}<0$) favors the local increase of perturbation energy in moist atmosphere and triggers the unstable development of mesoscale system. The divergent wave-activity flux ($\nabla\cdot\boldsymbol{F}>0$) will decrease the perturbation energy and prevent mesoscale system from developing. If the zonal basic flow is westerly, the Coriolis force work exerted by perturbed northerly is favorable for the increase of pseudoenergy wave-activity density, whereas the Coriolis force work by perturbed southerly weakens pseudoenergy wave-activity density. However, the contribution from the terms of zonal basic flow shear and source or sink is a little complicated. For a closed volume on whose boundaries the components of velocity vanish, the integration of Eq. (28) may be given by

$$\frac{\rm d}{{\rm d}t}\int\!\!\int_V\!\!\int A{\rm d}V$$
$$=\int\!\!\int_V\!\!\int\Big[u_0\Big(\frac{\partial\rho_0u_{\rm e}v_{\rm e}}{\partial y}+\frac{\partial\rho_0u_{\rm e}w_{\rm e}}{\partial z}\Big)-\rho u_0fv_{\rm e}$$
$$+\rho\Big(\frac{T_v}{T}\frac{Q}{c_p}+\lambda TS_{q_v}\Big)\Big(\frac{\partial C}{\partial\theta_v}\frac{\theta_v}{T_v}+c_p\Big)\Big]{\rm d}V.\qquad(29)$$

In the derivation of the above equation, the transformation relation

$$-\rho_0u_{\rm e}\Big(v_{\rm e}\frac{\partial u_0}{\partial y}+w_{\rm e}\frac{\partial u_0}{\partial z}\Big)=-\Big(\frac{\partial\rho_0u_0u_{\rm e}v_{\rm e}}{\partial y}+\frac{\partial\rho_0u_0u_{\rm e}w_{\rm e}}{\partial z}\Big)+u_0\Big(\frac{\partial\rho_0u_{\rm e}v_{\rm e}}{\partial y}+\frac{\partial\rho_0u_{\rm e}w_{\rm e}}{\partial z}\Big)$$

has been used. It can be seen from Eq. (29), the perturbation energy in a closed volume depends on the divergence of perturbation zonal momentum flux, Coriolis force work and source or sink. In the basic westerly, the divergent perturbation zonal momentum flux promotes mesoscale system, while the convergent perturbation zonal momentum flux decreases mesoscale system.

For adiabatic and dry atmosphere (namely, $Q=0$ and $S_{q_v}=0$), Eqs. (28) and (29) are transformed into the following

$$\frac{\partial A}{\partial t}+\nabla\cdot\boldsymbol{F}=-\rho_0u_{\rm e}\Big(v_{\rm e}\frac{\partial u_0}{\partial y}+w_{\rm e}\frac{\partial u_0}{\partial z}\Big)-\rho u_0fv_{\rm e},\ (30)$$

$$\frac{\rm d}{{\rm d}t}\int\!\!\int_V\!\!\int A{\rm d}V=\int\!\!\int_V\!\!\int\Big[u_0\Big(\frac{\partial\rho_0u_{\rm e}v_{\rm e}}{\partial y}+\frac{\partial\rho_0u_{\rm e}w_{\rm e}}{\partial z}\Big)-\rho u_0fv_{\rm e}\Big]{\rm d}V.\qquad(31)$$

It can be seen from the above two equations that when the zonal basic flow is constant ($u_0=c$), the

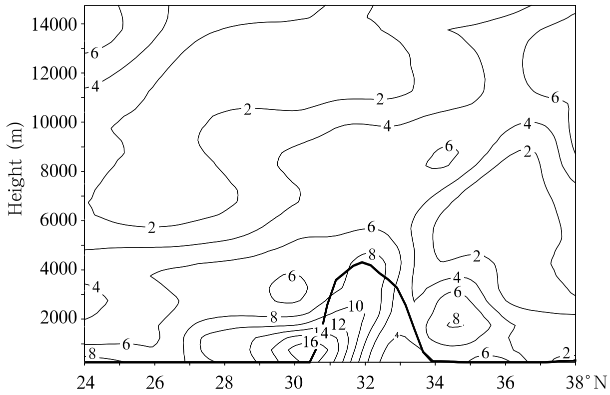

Fig. 1. The meridional-vertical cross-section of pseudoenergy wave-activity density (10 kg m^{-1} s^{-2}) zonally averaged between 118° and 121°E at 0000 UTC 5 July 2003. The thick solid line denotes the observed 6-h accumulated surface rainfall (mm) zonally averaged over the same longitude belt.

pseudoenergy wave-activity density is still nonconservative in global sense, and the tendency of A depends only on the Coriolis force work. Only when $u_0 = 0$, is the pseudoenergy wave-activity density conservative.

In conclusion, mesoscale system in stable-stratified atmosphere may be either local stable or unstable, which can be judged from the perspective of covariance of wave-activity flux divergence, zonal basic flow shear, Coriolis force work, and source or sink.

4. Case study

During the first ten days of July 2003, there often occurred rainstorms over the Yangtze and Huai River basins, and torrential rainfall events happened in some local areas. All these caused the most severe flooding disaster over these areas since 1991, bringing about great economic losses. In this section, a heavy rainfall event, which happened in the period of 0000 UTC 4–1200 UTC 5 July 2003, was diagnosed in virtual of pseudoenergy wave-activity relation Eq. (28). The analysis data used here came from the combination of NCEP/NCAR reanalysis data and routine surface and sounding observations by ADAS module of the ARPS

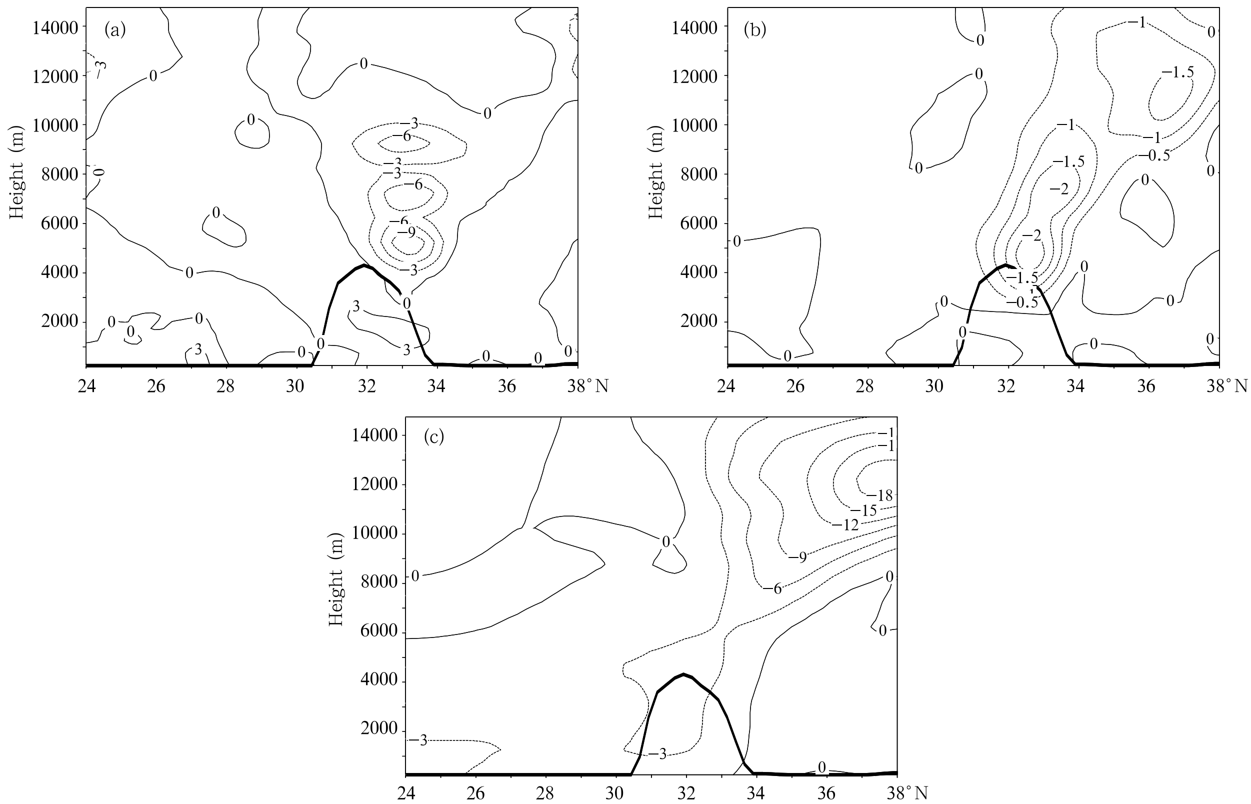

Fig. 2. Meridional-vertical cross-sections of (a) wave-activity flux divergence, (b) zonal basic flow shear, and (c) Coriolis force work zonally averaged between 118° and 121°E at 0000 UTC 5 July 2003 (unit: 10^{-3} Pa s^{-1}). The thick solid line denotes the observed 6-h accumulated surface rainfall (mm) zonally averaged over the same longitude belt.

accumulative rainfall was located in the latitude belt of 30.5°–34°N at 0000 UTC 5 July 2003. Below 3-km height, the positive high-value areas of pseudoenergy wave-activity density lay at both sides of the rain band. The positive-value areas on the southern side inclined northward and upward, strode over the rain band in the mid-lower troposphere and extended to the north of 38°N in the upper troposphere. The analysis also showed that the positive high-value areas on the southern side were due largely to the anomalies of available potential energy.

Figure 2 shows that the wave-activity flux converged below 3-km height over the rain band, indicating the convergence of wave-activity flux was beneficial to the increase of the pseudoenergy wave-activity density and the vigor of the perturbation system. The divergent wave-activity flux extended vertically from 3- to 12-km height, indicating that the divergence of wave-activity flux was prone to weaken the wave-activity density and inhibit development of the perturbation system. The large negative-value areas of the zonal basic flow shear, which inclined northward and upward above 3-km height over the rain band and extended to the north of 37°N, was unfavorable for the increase of pseudoenergy wave-activity density. Compared with the zonal basic flow shear, the wave-activity flux divergence was larger in magnitude. The Coriolis force work was negative and it inhibited the pseudoenergy wave-activity density. Its negative-value areas inclined northward and upward and arrived its maximum strength in the upper troposphere north of 34°N, in association with the upper-level jet stream.

The horizontal distribution of the observed 6-h accumulated surface rainfall at 0000 UTC 5 July 2003 displayed a band form with a northeast-southwest orientation (Fig. 3). The main part of the rain band extended from the southwest of Sichuan Province, via the middle of Hubei Province, to the middle and southern Zhejiang Province. The rainfall center was located at about 32°N, 119°E. The positive high-value pseudoenergy wave-activity density, vertically integrated from 3.25- to 7.25-km height, also appeared in the northeast-southwest direction and almost coincided with the rain band. The positive high-value area (30.5°–32.5°N, 116°–120°E) of pseudoenergy wave-activity density corresponded to the heavy-rainfall area. Additionally, above the rain areas, the column wave-activity flux divergence, zonal basic flow shear, and Coriolis force work were mostly negative (Fig. 4). Moreover, the negative high-value areas of wave-activity flux divergence and zonal basic flow shear were both situated near the heavy rainfall area. This implies that the wave-activity flux divergence and the terms of zonal basic flow shear and Coriolis force work were inclined to decrease the pseudoenergy wave-activity density and inhibit the development of perturbation systems.

From 0000 UTC 4 July to 1200 UTC 5 July (Fig. 5), the observed 6-h accumulated rainfall zonally averaged between 118° and 121°E moved gradually southward to 31°–33.5°N, and the positive high-value area of pseudoenergy wave-activity density (zonally averaged over the same longitude belt and vertically integrated from 3.25- to 7.25-km height) covered the heavy rainfall area and shared a similar pattern with the heavy rainfall. In Fig. 6, the heavy rainfall areas were overlapped by the negative-value areas of the wave-activity flux divergence, zonal basic flow shear, and Coriolis force work. The wave-activity flux divergence and the zonal basic flow shear shared the same

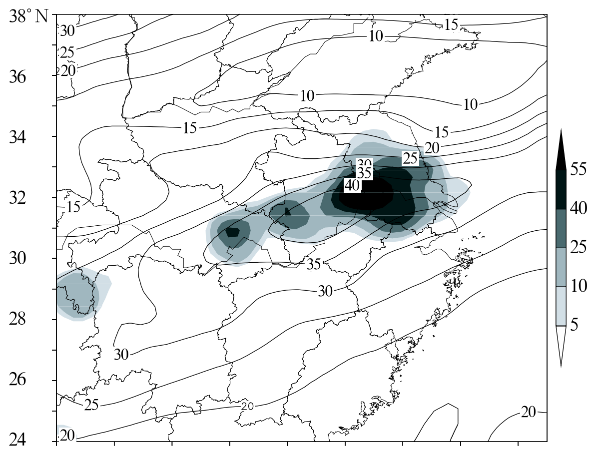

Fig. 3. The horizontal distribution of pseudoenergy wave-activity density (10^4 kg s^{-2}) vertically integrated from 3.25 to 7.25 km at 0000 UTC 5 July 2003. Shadings denote the observed 6-h accumulated surface rainfall (mm).

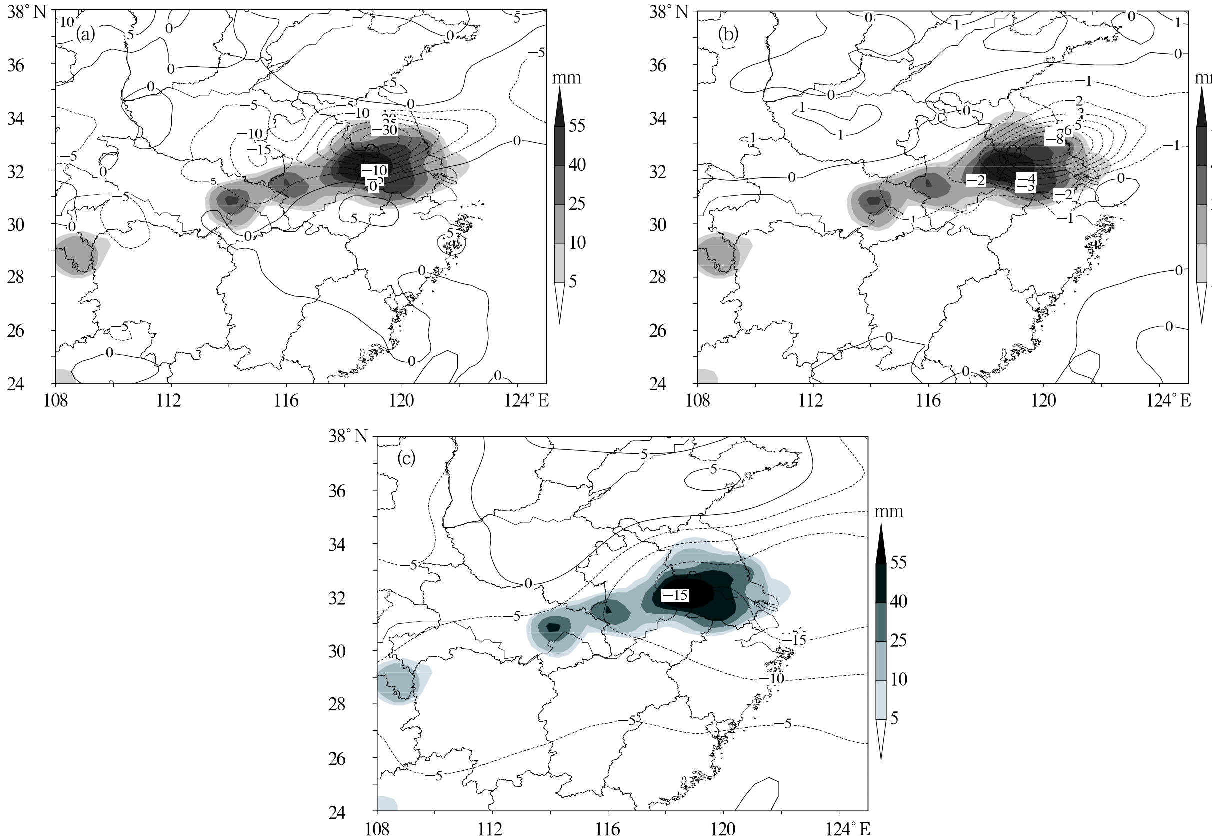

Fig. 4. Horizontal distributions of (a) wave-activity flux divergence, (b) zonal basic flow shear, and (c) Coriolis force work vertically integrated from 3.25 to 7.25 km at 0000 UTC 5 July 2003 (unit: Pa m s^{-1}). Shadings denote the observed 6-h accumulated surface rainfall (mm).

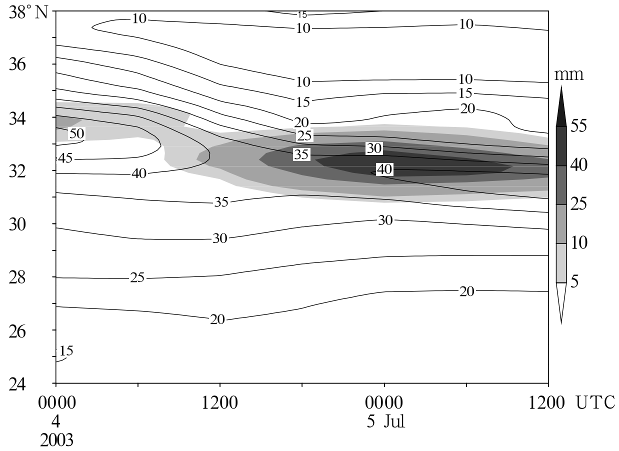

Fig. 5. The temporal-vertical cross-section of pseudoenergy wave-activity density (10^4 kg s^{-2}) zonally averaged between 118° and 121°E and vertically integrated from 3.25 to 7.25 km in the period of 0000 UTC 4–1200 UTC 5 July 2003. Shadings denote the observed 6-h accumulated surface rainfall (mm) zonally averaged over the same longitude belt.

temporal tend with the heavy rainfall. Near the heavy rainfall areas, the wave-activity flux divergence was more intensive than the zonal basic flow shear and Coriolis force work.

It can be seen from the above analysis that the pseudoenergy wave-activity density can reflect the dynamic and thermodynamic features of the mesoscale disturbance system leading to heavy rainfall in the mid-lower troposphere. So the density may indicate the evolution of precipitable systems and was closely related to surface heavy rainfall. In addition, the div ergence of wave-activity flux was similar to the temporal variation of pseudoenergy wave-activity density and was stronger than the zonal basic flow shear and Coriolis force work in magnitude, which indicates that the divergence of wave-activity flux made a significant contribution to the evolution of pseudoenergy wave-activity density.

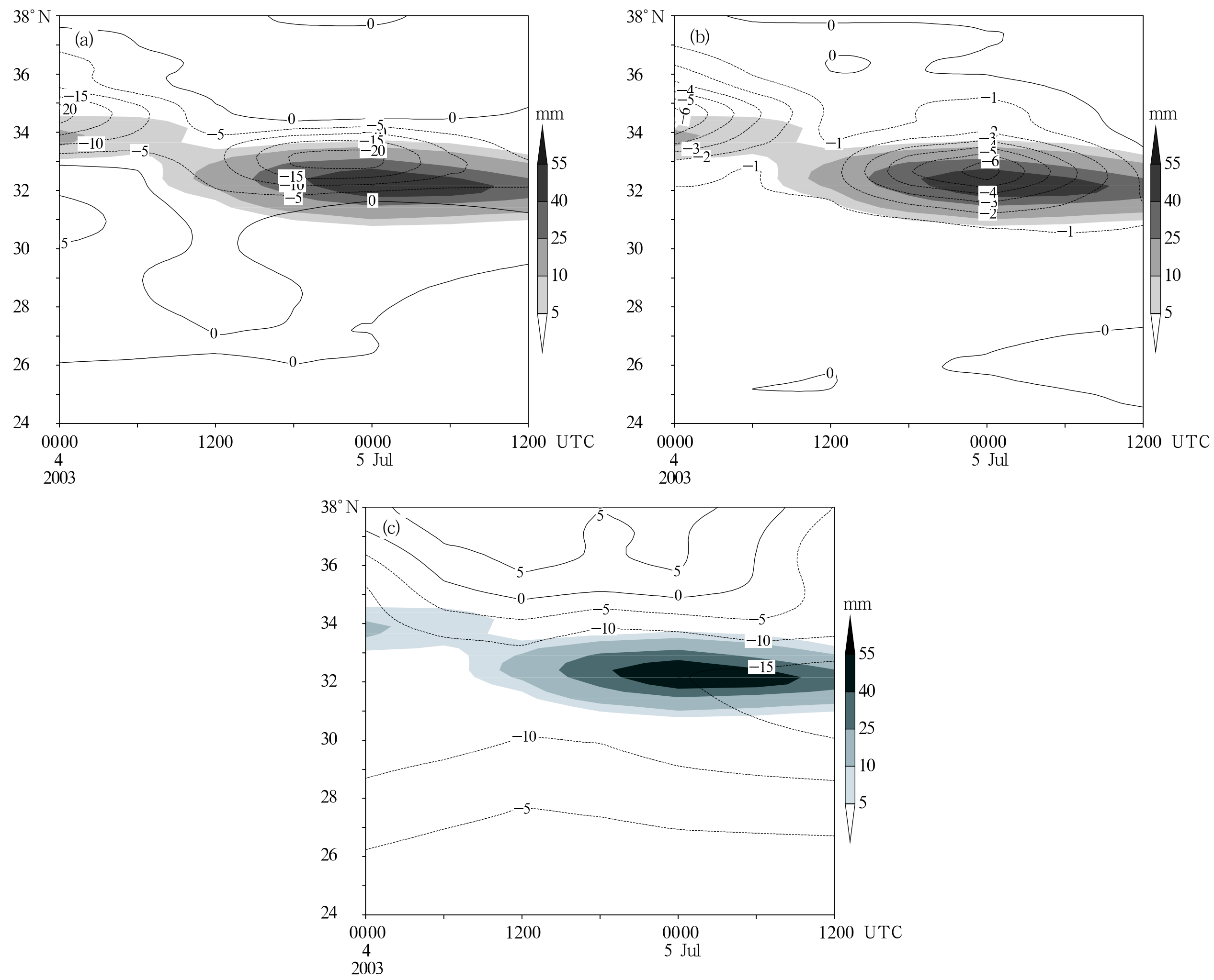

Fig. 6. Latitude-time cross-sections of (a) wave-activity flux divergence, (b) zonal basic flow shear, and (c) Coriolis force work zonally averaged between 118° and 121°E and vertically integrated from 3.25 to 7.25 km in the period of 0000 UTC 4–1200 UTC 5 July 2003 (unit: Pa m s^{-1}). Shadings denote the observed 6-h accumulated surface rainfall (mm) zonally averaged over the same longitude belt.

5. Conclusion

The condition of steady stratification in real atmosphere is usually satisfied, however, why can mesoscale systems still develop sharply? Can it be explained from the dynamic perspective of wave-basic flow interaction? To answer the questions, the pseudoenergy wave-activity relation suitable for mesoscale systems was derived with the energy-Casimir method, and favorable conditions for evolution of mesoscale systems were also discussed in this paper. Theoretical analysis showed that the wave-activity flux divergence and the terms of zonal basic flow shear, Coriolis force work, and source or sink of water vapor in the steady-stratified atmosphere made contributions to the tendency of pseudoenergy wave-activity density. For dry, adiabatic, and steady-stratified atmosphere, the tendency of pseudoenergy wave-activity density was subject to a local conservative law when the zonal basic flow was equal to zero.

The diagnosis of a heavy-rainfall event showed that the pseudoenergy wave-activity density shared a similar pattern in temporal variation with the observed 6-h accumulated surface rainfall. This indicates that the pseudoenergy wave-activity density in the mid-lower troposphere can prognose the mesoscale system leading to heavy rainfall to some degree. Although the wave-activity flux divergence and the terms of zonal basic flow shear and Coriolis force work were all prone to weaken the local change of pseudoenergy wave-acticity density, the wave-activity flux divergence made the most significant contribution than the other two terms.

REFERENCES

Arnol'd, V. I., 1965: Conditions for nonlinear stability of stationary plane curvilinear flows of an ideal fluid. *Dokl. Akad. Nauk. USSR*, **162**, 975–978. English Transl: *Soviet. Math.*, **6**, 773–777.

——, 1966: On a priori estimate in the theory of hydrodynamic stability. *Izv. Vyssh. Uchebn. Zaved, Matematika*, **54**, 3–5. EnglishTransl: *Am. Math. Soc. Transl. (Series 2)*, **79**, 267–269.

Charney, J. G., 1947: The dynamics of long waves in a baroclinic westerly current. *J. Meterr.*, **4**, 135–163.

Ding Yihui and Shen Xinyong, 1998: Symmetric instabilities of non-zonal and non-parallel mean flows. *Acta Meteor. Sinica*, **56**, 154–165. (in Chinese)

Eady, E. T., 1949: Long wave and cyclone waves. *Tellus*, **1**, 33–52.

Gao Shouting and Sun Shuqing, 1986: Determining the instability of mesoscale perturbations with Richardson number. *Scientia Atmos. Sinica*, **2**, 171–182. (in Chinese)

——, Tao Shiyan, and Ding Yihui, 1990: The generalized E-P flux of wave-mean flow interactions. *Science in China (Series B)*, **33**, 704–715.

Haynes, P. H., 1988: Forced, dissipative generalizations of finite-amplitude wave activity conservation relations for zonal and nonzonal basic flows. *J. Atmos. Sci.*, **45**, 2352–2362.

Huang Hong and Zhang Ming, 2008: Unstable dynamical properties of spiral cloud bands in tropical cyclones. *Acta Meteor. Sinica*, **23**(4), 485–493.

Kuo, H. L., 1949: Dynamic instability of two-dimensional non-divergent flow in a barotropic atmosphere. *J. Meteor.*, **6**, 105–122.

Li Yang and Mu Mu, 1996: Baroclinic instability in the generalized Phillips model. Part I: Two-layer model. *Adv. Atmos. Sci.*, **13**, 127–137.

Liu, Y. M., and Mu Mu, 1994: Arnol'd's second nonlinear stability theorem for general multi layer quasi-geostrophic model. *Adv. Atmos. Sci.*, **11**, 36–42.

Lu Weisong, 1989: On the nonlinear stability of shearing-basic flow in the frictional-dissipation atmosphere. *Acta Meteor. Sinica*, **47**, 412–423. (in Chinese)

McIntyre, M. E., and T. G. Shepherd, 1987: An exact local conservation theorem for finite amplitude disturbances to non-parallel shear flows, with remarks on Hamiltonian structure and on Arnol'd's stability theorems. *J. Fluid Mech.*, **181**, 527–565.

Mu Mu, 1991: Nonlinear stability criteria formotions of multi layer quasi-geostrophic flow. *Science in China (Ser. B)*, **34**, 1516–1528. (in Chinese)

——, 1992: Nonlinear stability of two-dimensional quasi-geostrophic motions. *Geophys. Astrophys. Fluid Dyn.*, **65**, 57–76.

——, 1998: Energy-Casimir method in the study of nonlinear stability of the atmospheric motions. *Advances in Mechanics*, **28**, 235–249.

——, and Zeng Qingcun, 1991: Criteria for the nonlinear stability of three-dimensional quasi-geostrophic motions. *Adv. Atmos. Sci.*, **8**, 1–10.

——, and X. Y. Wang, 1992: Nonlinear stability criteria for the motion of three-dimensional quasi-geostrophic flow on a beta-plane. *Nonlinearity*, **5**, 353–371.

——, V. Vladimirov, and Yong-Hui Wu, 1999: Energy-Casimir and energy-Lagrange methods in the study of nonlinear symmetric stability problems. *J. Atmos. Sci.*, **56**, 400–411.

Ren, S., 2000: Finite-amplitude wave-activity invariants and nonlinear stability theorems for shallow water semigeostrophic dynamics. *J. Atmos. Sci.*, **57**, 3388–3397.

Shen Xinyong, Ni Yunqi, Ding Yihui, and Wang Yu, 2007: Wave properties of mesoscale obliquely crossing instability and its numerical simulation. *Acta Meteor. Sinica*, **65**, 825–836. (in Chinese)

Stone, P. H., 1966: On non-geostrophic baroclinic stability. *J. Atmos. Sci.*, **23**, 390–400.

Zeng, Q. C., 1989: Variational principle of instability of atmospheric motion. *Adv. Atmos. Sci.*, **6**, 137–172.

Zhang Ying and Zhang Ming, 1995: The numerical research of symmetric instability. *Acta Meteor. Sinica*, **53**, 225–231. (in Chinese)

Zhou Yushu, Deng Guo, and Huang Yihong, 2003: Analysis on instability condition during a torrential rain over Yangtze River basin. *Acta Meteor. Sinica*, **61**, 323–333. (in Chinese)